Physics Letters B 739 (2014) 375–382

Contents lists available at ScienceDirect

Physics Letters B

www.elsevier.com/locate/physletb

Remarks on pole trajectories for resonances

C. Hanhart [a], J.R. Pelaez [b,*], G. Rios [c]

[a] Institut für Kernphysik, Institute for Advanced Simulations and Jülich Center for Hadron Physics, Forschungszentrum Jülich, 52425 Jülich, Germany
[b] Dept. Física Teórica II., Universidad Complutense, 28040 Madrid, Spain
[c] Helmholtz-Institut für Strahlen- und Kernphysik, Universität Bonn, D-53115 Bonn, Germany

ARTICLE INFO

Article history:
Received 4 August 2014
Received in revised form 6 November 2014
Accepted 10 November 2014
Available online 13 November 2014
Editor: J.-P. Blaizot

ABSTRACT

We discuss in general terms pole trajectories of resonances coupling to a continuum channel as some strength parameter is varied. It is demonstrated that, regardless of the underlying dynamics, the trajectories of poles that couple to the continuum in a partial wave higher than s-wave are qualitatively the same, while in case of s-waves the pole trajectory can reveal important information on the internal structure of the resonance. In addition we show that only molecular (or extraordinary) states appear near thresholds naturally, while more compact structures need a significant fine tuning in the parameters.
This study is of current relevance especially in strong interaction physics, since lattice QCD may be employed to deduce the pole trajectories for hadronic resonances as a function of the quark mass thus providing additional, new access to the structure of s-wave resonances.

1. Introduction

If all mesons were $\bar{q}q$ states then there would be no natural reason for poles in scattering amplitudes to occur very close to thresholds. At large values of N_c, the number of colors in QCD, all $\bar{q}q$ mesons become narrow with (nearly) unchanged mass [1]. Thus, their masses have no relation to the masses of the mesons to which they couple.[1] Accordingly, the ρ mass is not related to $2m_\pi$, nor is the K^* mass related to $m_K + m_\pi$. So the mere fact that the $f_0(980)$ and $a_0(980)$ appear very near $K\bar{K}$ threshold is already reason to be suspicious that they are not simple $\bar{q}q$ states. The same applies to unusual charmonium states that have been found near charm–anticharm meson thresholds like the famous $X(3872)$ located very close to the $D^0\bar{D}^{0*}$ threshold — for a recent review see [5].

On the other hand, there is good reason for "extraordinary" hadrons, often called hadronic molecules, to have masses close to thresholds [6]. In this paper we look carefully at the way that the manifestations of poles in scattering amplitudes change as the poles approach thresholds as some strength parameter is varied — here one may think of varying the quark masses in lattice QCD calculations. This has acquired a renewed interest after the trajectory of the σ or $f_0(500)$ resonance pole as a function of the quark mass was predicted by us within unitarized Chiral Perturbation Theory [7]. A similar trajectory as that of the σ was soon shown to be followed by the controversial κ or $K(800)$ resonance in the isospin 1/2 scalar πK scattering partial wave, including the appearance of a virtual state at sufficiently large pion masses [8]. The subtleties of the extraction of resonance parameters from lattice QCD simulations performed at a finite volume are outlined in detail in Refs. [9,10] and will not be discussed further here. Recently the existence of such a virtual bound state at high pion masses has been confirmed by lattice calculations [11].

While finishing this work, we became aware of a theoretical study [13] of the scaling of hadron masses near an s-wave threshold, showing that the bound state energy is not continuously connected to the real part of the resonance energy. In this paper we have another look at this issue which allows us to provide various additional, non-trivial insights. In particular, we demonstrate that there is a qualitative difference between the pole trajectories of resonances that couple to the relevant continuum channel in an s-wave or in a higher partial wave: As a consequence of analyticity a resonance is characterized by two poles on the second sheet, one located at $s = s_R$ and one located at $s = s_R^*$. For narrow resonances only one of them is close to the physical region. As some strength parameter is increased, the two poles start to approach each other. We demonstrate on general grounds below that while for higher partial waves the poles meet at the corresponding two meson threshold, for s-waves the poles can still be located inside the complex plane even for the real part of the

* Corresponding author.
E-mail address: jrpelaez@fis.ucm.es (J.R. Pelaez).

[1] The same is true for a straightforward extension of tetraquarks to large N_c [2] — in case they existed at large N_c [3] — although other possible extensions of tetraquarks to $N_c \neq 3$ lead to masses that grow when N_c is increased [4].

http://dx.doi.org/10.1016/j.physletb.2014.11.011

pole position at or below threshold. As a consequence, s-wave-trajectories are controlled by an additional dimensionful parameter, namely the value of s where the two poles meet below threshold which may be related to the structure of the state. In other words, generic trajectories of s-wave resonances do lead to poles whose real part of the position is below threshold, but whose imaginary part of the position does not vanish, before giving rise to virtual bound states, and then bound states, as some strength parameter is varied. While this observation is in line with the findings of Refs. [7,14], it is in vast conflict with "common wisdom" that the imaginary part of a pole has to be identified with one half of its decaying width, for this implies that, if the "resonance mass" — identified with the real part of the pole position — lies below threshold, the pole necessarily has to lie on the real axis.

The paper is organized as follows: in the next section we discuss general properties of the poles that appear in the S-matrix, paying particular attention to poles that occur in partial waves with angular momenta higher than 0, especially to the role of the centrifugal barrier which is absent in the scalar partial waves. Next we consider the trajectories of resonance poles in the complex plane as a function of some strength parameter, and how they can become bound states. In the next section we briefly review Weinberg's compositeness criterion and reformulate it in terms of the parameters introduced in the previous section. The possible behaviors are then illustrated with two models of scattering in separable potentials within non-relativistic scattering theory, one with a single channel and another one in a two-channel system. In Section 4 we analyze, the realistic examples of the pole trajectories of the σ or $f_0(500)$ scalar meson and the $\rho(770)$ as functions of the quark masses, obtained from the combination of Chiral Perturbation Theory and a single channel dispersion relation obtained in [7]. We show how the generic features discussed in this paper show up in these two cases. In particular, we can conclude that the $f_0(500)$ or sigma meson would have a predominantly molecular nature, if the pion mass were of the order of 450 MeV or higher. In the final section we summarize our results.

2. General properties of S-matrix poles

In this work we only consider one continuum channel. This implies that the S-matrix has one right hand cut, starting at $s = (2m)^2$ — the so-called unitarity cut.[2] As a consequence there are two sheets and, as usual, we call first or physical sheet the one corresponding to a momentum with a positive imaginary part. The S matrix evaluated on sheet I (II) is written as $S_I(s)$ ($S_{II}(s)$). If no subscript is given, the expression holds for both sheets. It follows directly from unitarity and analyticity that [15]

$$S_I(s) = 1/S_{II}(s) \quad \text{and} \quad \big[S(s)\big]^* = S\big(s^*\big). \tag{1}$$

As a consequence a pole on the second sheet immediately implies a zero on the first and vice-versa. In addition, if there is a pole at $s = s_0$, there must also be a pole at $s = s_0^*$, i.e., poles outside the real axis occur in conjugate pairs. Furthermore, it can be shown that the only poles allowed on the physical sheet are bound state poles, namely, those located on the real axis below threshold.

A different, but equivalent, way to discuss the pole structure of the S-matrix is to use the k-plane: instead of the Mandelstam variable s, the center of mass momentum k is used to characterize the energy of the system. The two quantities are related via

$$k = \sqrt{s/4 - m^2}. \tag{2}$$

[2] For simplicity we only consider the case of scattering of two particles with equal mass, however, the generalization to unequal masses is straightforward.

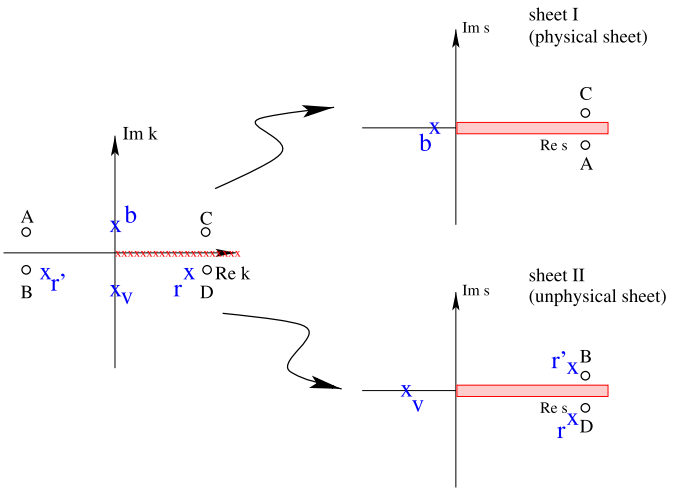

Fig. 1. Relation between k-plane and s-plane: on the left the k-plane is shown. The (red) xs denote the physical axis. On the right the two s-plane sheets are shown. Here the broad band indicates the position of the unitarity cut. The upper (lower) half plane of the k-plane maps onto the first (second) sheet in the s-plane such that the points A–D get transferred as indicated in the figure. In addition, the allowed pole positions in the complex plane are also shown as x. They are labeled as b for the bound state, v for the virtual state, and r and r' for the two conjugate poles of the resonance state.

The obvious advantage is that there is no right hand cut with respect to k and correspondingly there is only one sheet. It follows directly from the definition that the upper (lower) half plane of the complex k-plane, defined by positive (negative) values of the imaginary part of k, maps onto the first (second) sheet of the s-plane. The conditions derived above from Eq. (1) translate into the k-plane as follows: the only poles allowed in the upper half plane are on the imaginary axis and in the lower half plane appear as mirror images with respect to the imaginary axis. The relation between the different planes is illustrated in Fig. 1. On the one hand, it becomes clear from the figure that the resonance pole located at r is the one closest to the physical axis and therefore physically more relevant than the one at r' in the vicinity of the pole. On the other hand, at the threshold both poles are equally relevant regardless where they are located in the second sheet. Finally, in the k plane virtual states appear as poles on the negative imaginary axis (labeled as v in the figure) and bound states as poles on the positive imaginary axis (labeled as b in the figure).

Now, assuming that there is at least one resonance pole, and that it is not too far away from threshold, we are now in the position of writing down the most general expression for the S-matrix in the vicinity of that pole or its conjugate partner. For the derivation it is easier to use the k plane, and thus we assume that there is a resonance pole at $k = k_{\rm p} - i\gamma$ with $\gamma > 0$. For a resonance, $k_{\rm p}$ is a real number and we choose $k_{\rm p} > 0$, for, as commented above, it corresponds to the pole closest to the physical axis. Then, from the above considerations it follows that there is in addition a pole at $k = -k_{\rm p} - i\gamma$ and zeros at $k = \pm k_{\rm p} + i\gamma$. We may therefore, dropping terms of higher order in k, and for a particular partial wave ℓ, write the following general expression for the S-matrix element in the vicinity of the pole [15]:

$$S_\ell(k) = e^{i\phi(k)}\,\frac{(k - k_{\rm p} - i\gamma)(k + k_{\rm p} - i\gamma)}{(k - k_{\rm p} + i\gamma)(k + k_{\rm p} + i\gamma)}, \tag{3}$$

where $\phi(k)$ is a smooth function, real valued for real, positive values of k. For simplicity this phase factor will be dropped in what

follows. Using the definition of the T matrix, $S = 1 + 2ikT$, we may write

$$T_\ell(k) = -\frac{2\gamma}{k^2 - (\gamma^2 + k_{\rm p}^2) + 2i\gamma k}. \tag{4}$$

For elastic scattering unitarity provides a stringent link between the real and the imaginary part of T, that actually allows the T-matrix elements to be described in terms of its phase δ as

$$\tan(\delta) = -\frac{2k\gamma}{k^2 - (\gamma^2 + k_{\rm p}^2)}. \tag{5}$$

Of course, it is straightforward to recast the above expressions in terms of s instead of k. One finds for example

$$S_\ell(k) = \frac{s - s_0 - 4i(s-4m^2)^{1/2}\gamma}{s - s_0 + 4i(s-4m^2)^{1/2}\gamma}, \tag{6}$$

with $s_0 = 4(k_{\rm p}^2 + \gamma^2 + m^2)$.

2.1. $\ell > 0$ partial wave threshold behavior and poles

In general the centrifugal barrier demands, for momenta much smaller than some typical scale μ, that the scattering amplitude behaves as $T_\ell \propto k^{2\ell}$. If we are only interested in this low energy region, the constraint translates into the replacement

$$\gamma \to \gamma(k) = \bar\gamma k^{2\ell}. \tag{7}$$

Of course, this amplitude should only be used for k much smaller than the typical scale μ, not beyond. Note that $\ell = 0$ waves are unaffected by this change, but, for example, $\ell = 1$ waves now have poles whenever $i\bar\gamma k^2 + k \pm k_{\rm p} = 0$, namely at:

$$k_{\rm pole} = \frac{i}{2\bar\gamma}\left[1 \pm \sqrt{1 \mp 4i\bar\gamma k_{\rm p}}\,\right], \quad (\ell = 1 \text{ case}). \tag{8}$$

These are four poles in conjugated pairs, but of course, they are only meaningful if they lie within the low momentum region of validity of our amplitude. We can ensure that we have only one conjugated pair within this region, if we require $\bar\gamma k_{\rm p} \ll 1$, (which is nothing but assuming that both parameters are natural, i.e., $\bar\gamma \ll 1/\mu$ and $k_{\rm p} \ll \mu$). In such case we can expand

$$\sqrt{1 \mp 4i\bar\gamma k_{\rm p}} \simeq 1 \mp 2i\bar\gamma k_{\rm p} + 2\bar\gamma^2 k_{\rm p}^2 + \cdots, \tag{9}$$

so that the four poles lie at:

$$\begin{aligned} k_{\rm pole} &\simeq \frac{i}{2\bar\gamma}\left[1 \pm \left(1 \mp 2i\bar\gamma k_{\rm p} + 2\bar\gamma^2 k_{\rm p}^2\right)\right] \\ &= \begin{cases} \mp k_{\rm p} - i\bar\gamma k_{\rm p}^2 & \text{(physical pair)} \\ \pm k_{\rm p} + \frac{i}{\bar\gamma}(1 + (\bar\gamma k_{\rm p})^2) & \text{(unphysical pair)} \end{cases} \end{aligned} \tag{10}$$

One should not worry about the unphysical conjugated pair of poles lying on the first sheet, since our amplitude has been constructed for $1/\bar\gamma \gg k_{\rm p}$ and thus these spurious poles are deep in the complex plane, beyond the range of applicability of our approach, which is however valid for the two poles not too far from threshold. A similar pattern emerges for even higher partial waves, with a physical pair for small k and additional unphysical pairs of poles beyond the applicability region of our amplitude.

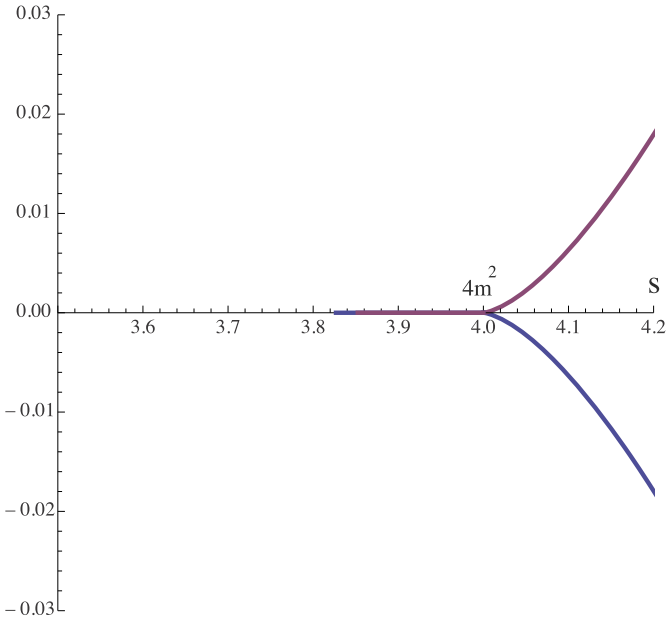

Fig. 2. Motion of the p-wave poles in the complex s-plane with $m = 1$ and $\bar\gamma = 0.2$.

2.2. Pole trajectories as a function of a strength parameter

In the construction presented in the previous section it was assumed that $k_{\rm p}$ is a real number — then the equations describe a resonance. We will now generalize this investigation by considering the movement of the poles as some strength parameter is varied. Therefore we will study how the resonance properties change when varying $k_{\rm p}$. In particular, it is interesting to observe the trajectories of the poles for $k_{\rm p} \to 0$ especially very close to threshold. Of course, as long as two conjugate poles exist, their trajectories have to be symmetric with respect to the imaginary k axis.

Let us first follow the trajectories of conjugate poles for $\ell > 0$ partial waves. As a consequence of Eq. (7), they will come infinitesimally close to $k_{\rm pole} = 0$. However, as commented above there can be no poles of the S-matrix on the physical cut. This property is automatically implemented in Eq. (3) for when $k_{\rm p} = 0$ and $\gamma = 0$ simultaneously, the zeros in the numerator and denominator cancel to yield $S(k = 0) = 1$. The resulting pole trajectories in the s plane are illustrated for $\ell = 1$ in Fig. 2.

In contrast, for s-waves the point where the two conjugate poles meet each other on the imaginary k axis is not fixed except for the condition that no poles in the physical axis should exist in the first Riemann sheet, and in particular not at $k = 0$. But that leaves the whole negative axis for s-wave poles to meet when $k_{\rm p}$ decreases and the point where the two trajectories meet, $-i\gamma$, is a non-trivial parameter of the underlying dynamics. This is one of the central messages of this paper.

In order to extend our discussion to poles below threshold, we need to continue analytically $k_{\rm p}$ to complex values $k_{\rm p} = i\kappa_{\rm p}$, with $\kappa_{\rm p}$ real and positive so that $k_{\rm p}^2$ is real and negative. Of course, for our amplitude to make sense we still keep the condition $\bar\gamma\kappa_{\rm p} \ll 1$.

Now, for the $\ell > 0$ case, we find two physical poles at $k_{\rm pole} = i\kappa_{\rm p}(\pm 1 + \bar\gamma\kappa_{\rm p})$. In the s-plane, these are two poles below threshold but one in the first and another one in the second Riemann sheet. The resonance has become a bound state. Since $\bar\gamma\kappa_{\rm p} \ll 1$ they lie almost symmetrically with respect to the threshold. As seen from the s-plane, this is the typical structure of subthreshold poles in the first and second Riemann sheets.

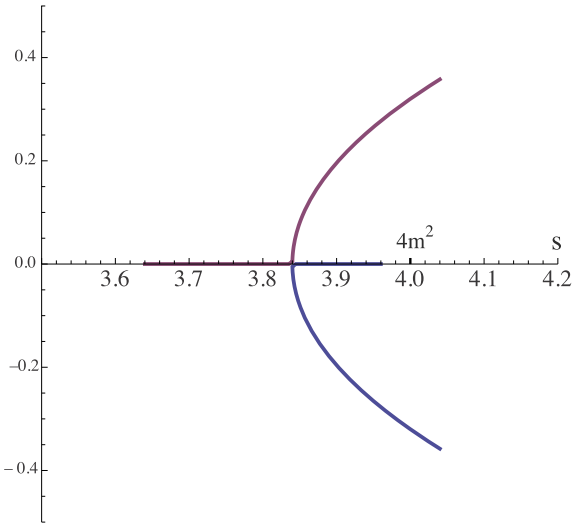

Fig. 3. Motion of the s-wave poles in the complex s-plane with $m = 1$ and $\gamma = 0.2$.

In contrast, for scalar waves, we find two poles in the imaginary axis at $k_{\text{pole}} = i(\pm\kappa_{\text{p}} - \gamma)$. Note that, as κ_{p} grows, the two poles start separating from each other and move apart from the "meeting point", $-i\gamma$. In the k-plane both move along the imaginary k-axis, the physically more relevant one is located at $-i(\gamma - \kappa_{\text{p}})$ while the other one is located at $-i(\gamma + \kappa_{\text{p}})$. Correspondingly in the s-plane the two poles move along the negative real axis, but both of them lying on the second sheet until $\kappa_{\text{p}} = \gamma$. Eventually, when $\kappa_{\text{p}} > \gamma$, the first pole moves to the physical sheet — the virtual state turns into a bound state.[3] The corresponding motion of the poles is illustrated in Fig. 3.

One may define the mass M of a particle as the real part of the corresponding pole position in the complex plane. It is therefore interesting to follow this point as γ and k_{p} vary. For s-waves, in general one finds a striking non-analytic behavior in M at the point where $k_{\text{p}} = 0$. On the other hand, for partial waves higher than s-waves the behavior is much smoother.[4] This non-analyticity of the hadron mass when the conjugate poles reach the real axis as $k_{\text{p}} \to 0$ has been recently studied in detail within the general formalism of Jost functions in [13]. The conclusion is a similar warning to the one we raised in Ref. [7] about the naive mass extrapolation formulas for states which appear near thresholds on the lattice, although within a more general framework. In this work we will illustrate this non-analyticity in passing, when explaining the different possible pole trajectories on the basis of various examples below, whereas for the analytic formalism of those mass singularities we simply refer the reader to [13].

3. Summary of Weinberg's criterion

In Ref. [17] Weinberg developed a criterion for compositeness for bound states that occur in the s-wave of scattering amplitudes (under which circumstances this formalism can be generalized to resonances is described in Ref. [18]). The starting point is the scattering amplitude near threshold that may be expressed in terms of the scattering length, a, and the effective range, r as[5]

$$T_0(k) = \frac{1}{k\cot\delta_0(k) - ik} = \frac{1}{-1/a + rk^2/2 - ik}. \tag{11}$$

Weinberg derived relations between the scattering length, a, the effective range, r, and the wave function renormalization constant for the particle described by the S-matrix pole, Z,

$$a = 2\left(\frac{1-Z}{2-Z}\right)R + \mathcal{O}(1/\beta),$$
$$r = -\left(\frac{Z}{1-Z}\right)R + \mathcal{O}(1/\beta). \tag{12}$$

Here β is the typical momentum scale of the binding interactions — in our case either $\beta \sim m_\pi$ or larger, depending on whether single pion exchange is important in the process — and R is the inverse of the imaginary momentum corresponding to the S-matrix pole

$$R = \frac{1}{\kappa} = \sqrt{\frac{1}{mB}} \tag{13}$$

when the pole in S occurs at $s = 4(m^2 - \kappa^2) = 4m^2 - 4mB$. For a bound state $\kappa > 0$ and for a virtual state $\kappa < 0$ (in both cases $B > 0$). On general grounds one can show for bound states that to leading order in a $1/(R\beta)$ expansion, Z can be interpreted as the probability to find the ordinary, compact component in the wave function of the physical state. In particular, $0 \le Z \le 1$ [17].[6]

Assuming that the effective range approximation is valid for all momenta of interest, from Eq. (11) evaluated at the pole follows a single kinematic relation among a, r, and R

$$\frac{1}{R} = \frac{1}{a} + \frac{r}{2R^2} \tag{14}$$

Weinberg found that a predominantly composite state (or hadronic molecule or extraordinary hadron) has $Z \approx 0$. In the case of a weakly bound particle, where $R \gg 1/\beta$, this criterion reduces to $a \sim R$ and $r \sim 1/\beta$, with the range term in Eq. (14) just providing a small correction. Note that within potential scattering one can show that the terms of order $1/\beta$ are typically positive.

On the other hand, a predominantly elementary state has $Z \approx 1$ and therefore $a \sim 0$, or more accurately $a \sim 1/\beta \ll R$, and $|r| \gg R$. As a result, in order to get a bound state near threshold for a predominantly elementary state a fine tuning between the range term and the scattering length term is necessary in Eq. (14).[7] This clearly demonstrates, that it is way more natural to find composite states near thresholds than elementary states.

The effective range parameters can easily be expressed in terms of the parameters introduced in the previous section. From Eq. (4) one finds

$$a = -\frac{2\gamma}{\gamma^2 + k_{\text{p}}^2} = \frac{2\gamma}{\kappa_{\text{p}}^2 - \gamma^2} \quad \text{and} \quad r = -\frac{1}{\gamma}, \tag{15}$$

where we used that for bound states k_{p} gets imaginary. Using Eq. (12) this can be translated to

$$Z = 1 - \frac{\gamma}{\kappa_{\text{p}}}. \tag{16}$$

[3] A similar pole movement from the first to the second Riemann sheet through threshold has been found in a scalar field propagator within a simple model where it couples to two pseudoscalar fields [12].

[4] This non-analytical behavior in hadron masses may also propagate to other observables, like form factors in the t-channel [16].

[5] Note that some times a different sign convention is used for the scattering length.

[6] In Ref. [19] it was explicitly shown that such an interpretation dos not hold for virtual states.

[7] This situation may be accompanied by quite unusual line shapes as demonstrated in Refs. [21,22].

As explained in the previous section, for a shallow bound state one has $(\kappa_{\rm p}-\gamma)=\kappa\ll\beta$. The natural parameter range is $\kappa_{\rm p},\ \gamma\sim\beta$. We therefore again need to conclude that the most natural situation for a near threshold pole is $Z\simeq 0$ – only if both $\kappa_{\rm p}$ and γ are individually much smaller than β and at the same time $\gamma\ll\kappa_{\rm p}$, then $Z\simeq 1$, referring to an elementary state. Clearly, for this to be realized fine tuning is necessary.

Although unlikely to occur in nature, it is of theoretical interest to have a closer look at a pole with vanishing binding energy, $\kappa\to 0$. Without loss of generality we may now write

$$\gamma=\delta \quad\text{and}\quad \kappa_{\rm p}=(1+\epsilon)\delta.$$

With this we get

$$\kappa=\epsilon\delta,\qquad a=\left(\frac{2}{2+\epsilon}\right)\frac{1}{\kappa}\quad\text{and}\quad Z=\frac{\epsilon}{1+\epsilon}.$$

A vanishing binding energy ($\kappa\to 0$) can be achieved either by $\epsilon\to 0$ for finite δ, which implies $Z\to 0$ – the physical state is molecular. Alternatively it can also be achieved via $\delta\to 0$ – this is the fine tuning situation indicated above for it implies not only γ and κ to be equal (which is necessary and sufficient for the pole to be located at threshold), but both to vanish at the same point. If in this case at the same time ϵ is much larger than 1, the state is predominantly genuine. In general the scattering length diverges for $\kappa\to 0$, however, $a\kappa$ is finite and, as before, bounded from above for the pure molecule and decreasing with an increasing non-molecular admixture. The state becomes purely genuine in the $\epsilon\to\infty$ limit – where the resonant state located at the continuum threshold decouples completely from the continuum state.

In the following we will illustrate the patterns described above on two simple models. Some pole trajectories within a specific coupled channel model were shown in Ref. [20]. Both of these models are based on non-relativistic scattering in a separable potential. Model A is a single channel separable potential. If the potential is attractive and strong enough, it can generate an S-matrix pole. In [6] it was argued that this is a "toy model" for an extraordinary hadron which would vanish as $N_c\to\infty$. Model B is a two channel model where there is no diagonal interaction in the open channel, but there is a bound state in the closed channel (a Feshbach resonance). In [6] it was argued that this is a model for an "ordinary hadron", whose width would go to zero as $N_c\to\infty$.

3.1. Model A

Model A has a separable potential that only couples to a single partial wave with angular momentum l. The scattering amplitude in all other partial waves is zero. For the partial wave with angular momentum l, the Schrödinger equation is

$$-u_\ell''(r)+\frac{\ell(\ell+1)}{r^2}u_\ell(r)-\int_0^\infty dr' V(r,r')u_\ell(r')=Eu_\ell(r'),\qquad(17)$$

where we use a separable form for the potential

$$V(r,r')=\lambda v(r)v(r')\qquad(18)$$

To make things simple $v(r)$ is chosen such that the integrals can be done analytically:

$$v(r)=\sqrt{2}\mu^{3/2}e^{-\mu r}.\qquad(19)$$

Although for $r\sim 1/\mu$ the behavior of the system depends on the form chosen for $v(r)$, the behavior for $r\gg 1/\mu$ is genuine.

Then one finds for the scattering amplitude, $f_l(k)$,

$$f_l(k)=\frac{k\lambda\xi_l^2(k)}{1-\frac{2\lambda}{\pi}\int_0^\infty dqq^2\frac{\xi_l^2(q)}{q^2-k^2-i\epsilon}}\equiv\frac{N_l(k)}{D_l(k)},\qquad(20)$$

where $\xi_l(k)=\int_0^\infty rj_l(kr)v(r)$, and in particular

$$\xi_0(k)=\frac{\sqrt{2}}{k^2+\mu^2}.\qquad(21)$$

The model should reproduce the genuine behavior discussed above for $|k|\ll\mu$. One can compute $N(k)$ and $D(k)$ explicitly; for the s-wave ($\ell=0$),

$$N_0(k)=\frac{2\mu^3k\lambda}{(k^2+\mu^2)^2},$$
$$D_0(k)=1+\frac{\lambda\mu^2}{(k+i\mu)^2}.$$

For s-wave poles located near a threshold one may use Weinberg's criterion to pin down the degree of compositeness of the corresponding physical state. Here closeness to the threshold translates into $k\ll 1$. The relevant poles[8] are the zeros of $D_0(k)$ located at

$$k_{\rm p}=-i\mu(1\pm\sqrt{\lambda}).\qquad(22)$$

In addition we may read off from the expressions given above

$$a_A=\frac{2\lambda}{\lambda-1}\frac{1}{\mu}\quad\text{and}\quad r_A=\frac{\lambda+2}{\lambda}\frac{1}{\mu}.\qquad(23)$$

A bound state (pole on the positive imaginary axis) is present only for $\lambda>1$ ($\lambda<0$ refers to a repulsive interaction). In addition, r is always positive – which means that in Eq. (12) for the range the $1/\beta$ term dominates. Thus, the pole is located very near threshold only for $r_A/(2a_A)\ll 1$, as follows straightforwardly from Eq. (14) – within the model this ratio does not exceed 0.3 showing that Model A produces extraordinary hadrons in the whole parameter range where bound states are produced. Equivalently one may also directly calculate the wave function renormalization constant for the s-wave – one finds it consistent with 0 within the uncertainties. Thus, the single partial wave separable potential generates an S-matrix pole dynamically that mimics an extraordinary hadron: a hadronic molecule.

3.2. Model B

This model is designed to show the scattering effects of a confined state when it can be treated non-relativistically using the Schrödinger equation. It is described in detail in [6], Section II.C, and will not be repeated here. Basically it maps onto a separable potential model of Eq. (18) but with $\lambda\to\lambda/(E-E_0)$, where $E_0=k_0^2/m$ is the energy of the confined channel bound state renormalized by the interactions in the continuum channel – Feshbach showed that near such a state the two channel Schrödinger Equation collapses to a single channel equation with a separable potential. Here are the numerator and denominator of the s-wave scattering amplitude for this model:

$$N_0(k)=\frac{2k\mu^3\lambda}{(k^2+\mu^2)^2},\qquad(24)$$

$$D_0(k)=k^2-k_0^2+\frac{\lambda\mu^2}{(k+i\mu)^2}.\qquad(25)$$

[8] In this model also the numerator function develops poles, however, those are unphysical and outside the range of validity of the model identified at $|k|\ll\mu$.

The only difference between the two models is that the 1 in $D_0(k)$ in Model A is replaced by $k^2 - k_0^2$ in Model B — said differently: Model A is recovered from model B in the limit $k_0^2 \to -\infty$ while $\bar{\lambda} = -\lambda/k_0^2$ is kept finite. In particular, this implies that, in some areas of parameter space, model B describes, as model A, composite states. However, because of the new extra parameter, k_0, the location of a near threshold pole in the scattering amplitude is no longer necessarily linked to the scattering length and as a consequence Weinberg's criterion for compositeness can be evaded. To discuss in more detail the role of k_0 we may have a closer look at the effective range parameters in terms $\bar{\lambda}$:

$$a_B = \frac{2\bar{\lambda}}{\bar{\lambda}-1}\frac{1}{\mu} \quad \text{and} \quad r_B = \frac{\bar{\lambda}+2-\mu^2/k_0^2}{\bar{\lambda}}\frac{1}{\mu}. \tag{26}$$

As a consequence of causality the value of r_B is bounded from above [23][9] — thus small and positive values of $\bar{\lambda}$ lead to unphysical results as soon as $k_0^2 < 0$. On the other hand, as long as $\bar{\lambda}$ is negative we do get the situation of a scattering length of the order of the range of forces, especially independent of the binding energy, accompanied by a large and negative effective range as soon as k_0^2 tends to zero from the negative side, which refers to an ordinary or genuine state. The physics of this scenario is intuitively clear: if the coupling to the confined state is very weak or repulsive, it should appear like an elementary particle in the scattering channel. This is the case for negative $\bar{\lambda}$ and negative, small k_0^2. In particular one finds in this corner of parameter space for the pole locations (again using $k_0 = i\kappa_0$)

$$k_p = i\kappa_0\left(\pm\sqrt{1-\bar{\lambda}} + \bar{\lambda}\frac{\kappa_0}{\mu} + \mathcal{O}\left(\left(\frac{\kappa_0}{\mu}\right)^2\right)\right). \tag{27}$$

To get a state near threshold both κ_0 and $\bar{\lambda}$ must be small simultaneously. If one takes, for instance, $\bar{\lambda} = -0.1$ and $\kappa_0 = 0.3\mu$ one obtains a bound state with $Z \simeq 1$, which is to be interpreted as an elementary state.[10]

In summary, for certain parameters, that need to be fine–tuned considerably, the "Feshbach" resonance model can describe a bound state in a confined channel that couples to scattering in an open channel that does not satisfy Weinberg' criterion for compositeness and thus should be interpreted as a genuine ("ordinary") state.

At the end of this section we again briefly turn to the special case of a state located exactly at threshold. In case of Model A (or equivalently Model B with $k_0^2 \to -\infty$ while $\bar{\lambda} = -\lambda/k_0^2$ is kept finite) the pole is located exactly at threshold for $\lambda = 1$. In this case the scattering length diverges and r_B is of order of the range of forces. On the other hand, to produce a genuine state exactly at threshold within Model B we need to take the limit $k_0^2 \to 0_-$ accompanied by a negative value for $\bar{\lambda}$. Then indeed we formally get a pole at threshold with a scattering length of the order of the range of forces and infinite, negative effective range, but at the same time the full scattering amplitude vanishes as already discussed in Section 3. Thus in the mathematical limit of a state located exactly at threshold in the presence of purely elastic interactions the state is necessarily of molecular nature. One might thus be tempted to argue that a genuine pole exactly at threshold is not possible. However, most candidates for molecular states recently discovered in the heavy meson sector were first discovered not in the continuum channel were the state might have been formed

[9] A proof of the Wigner bound that does not assume the potential to be local is given in [24].

[10] Again we omitted poles outside the range of validity of the model from the discussion.

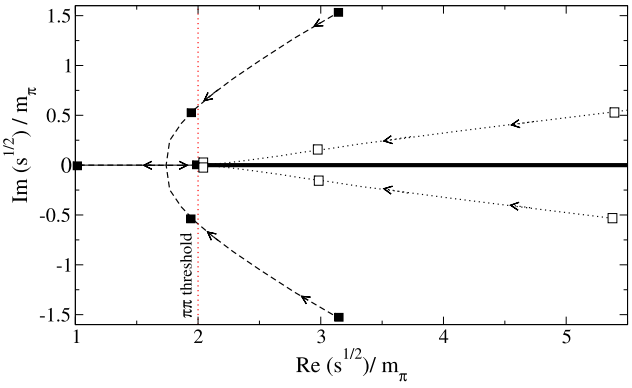

Fig. 4. Movement of the σ (dashed lines) and ρ (dotted lines) poles for increasing pion masses (direction indicated by the arrows) on the second sheet as extracted from the IAM. The filled (open) boxes denote the pole positions for the σ (ρ) at pion masses $m_\pi = 1, 2$, and $3 \times m_\pi^{\text{phys}}$, respectively. Note, for $m_\pi = 3m_\pi^{\text{phys}}$ three poles accumulate in the plot very near the $\pi\pi$ threshold.

but in other decay channels (e.g. the $X(3872)$, a candidate for a $D^*\bar{D}$ bound state, was discovered via its decay into $J/\psi\pi\pi$ [25]) and therefore the pole still shows up in the physical S-matrix. In addition, as soon as the binding energy is different from zero, no matter how small, the full analysis outlined in this paper applies.

4. A realistic example: pole trajectories of the σ and ρ mesons as a function of quark masses

In order to illustrate with a realistic example what was described in the previous sections, we now show the results for the pole trajectories of the ρ-meson and the σ-meson calculated within the inverse amplitude method (IAM) [26]. The approach uses Chiral Perturbation Theory (ChPT) predictions to a given order to fix the subtraction constants of an elastic partial wave dispersion relation. This leads to an amplitude consistent with elastic unitarity that by construction matches the ChPT expansion when re-expanded at low energies and at the same time generates the poles associated with the σ and ρ resonances in pion–pion scattering [27]. Note that the numerical values of the low energy constants obtained when fitting the IAM to scattering data might slightly differ from those of ChPT since they absorb higher order effects. Since the whole QCD quark mass dependence is included up to the desired order in terms of the ChPT expansion of the pion mass and decay constant, one can study the quark mass dependence of both the σ and ρ resonances [7]. In Fig. 4 we show the pole movement in the second sheet for both σ and ρ.

At this point we must recall that the IAM formalism contains the left cut singularity required by crossing symmetry in relativistic scattering. Note however that although the inverse amplitude discontinuity along the elastic right cut is calculated exactly in the IAM, along the left cut it is only approximated to one loop. In any case, this is an analytic structure that our simple model of the previous sections does not contain. Nevertheless, the effect is expected to be rather small for most of our parameter space, since, for most of our parameter space, both the σ and ρ poles lie far from this left cut which starts at $s = 0$ and extends to $-\infty$. Actually, for physical masses it has been shown that the sigma can be generated with a very similar formalism to that of the IAM, using leading order ChPT, but with no left cut at all [28]. However the approximations in that formalism do not allow to follow so nicely the mass dependence as with the IAM (since, among other issues, there is a cutoff).

Of course, it is clear that in cases when the pole moves closer to the left cut than to the physical one, our simple "isolated-pole near

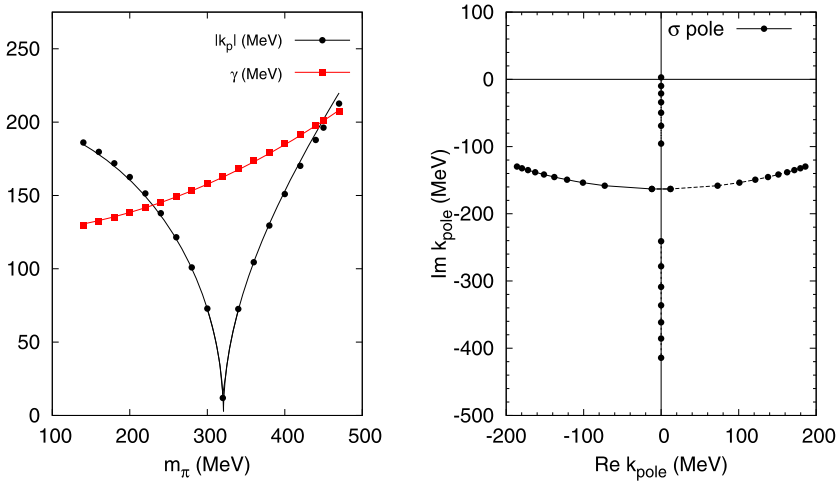

Fig. 5. Behavior of the σ pole in the k-plane. Left panel: m_π dependence of k_p and γ. The filled circles (boxes) show the results of the numerical determination for $|k_\mathrm{p}|$ (γ) from the full calculation, while the lines are produced from the fitting functions given in the text. Right panel: the resulting pole movement for the σ in the k-plane. The dots correspond to pion masses ranging from 140 MeV to 460 MeV in intervals of 20 MeV.

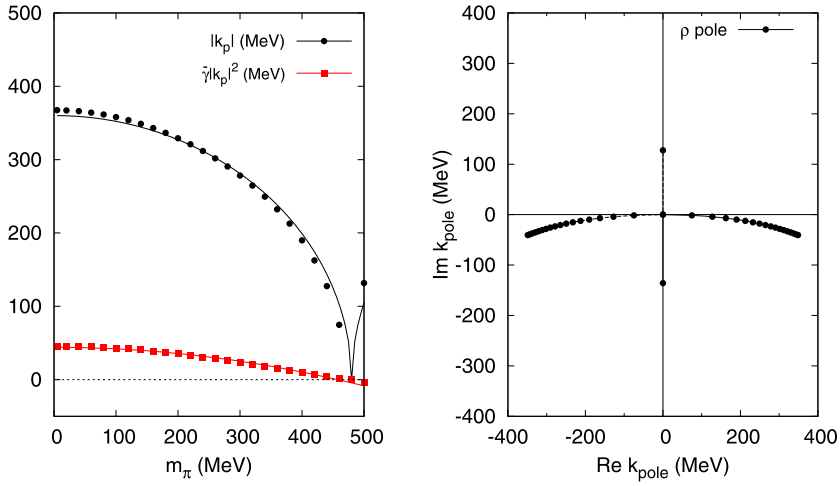

Fig. 6. Behavior of the ρ pole in the k-plane. Left panel: m_π dependence of k_p and $\tilde{\gamma}$. The filled circles (boxes) show the results of the numerical determination for $|k_\mathrm{p}|$ ($\tilde{\gamma} k_\mathrm{p}^2$) from the full calculation, while the lines are produced from the fitting functions given in the text. Right panel: the resulting pole movement for the ρ in the k-plane. The dots correspond to pion masses ranging from 140 MeV to 500 MeV in intervals of 20 MeV.

threshold" model would not hold. Fortunately, according to the results in [7], this never happens for the ρ, whose mass is always larger than 700 MeV for all the values of m_π under study. However, for values of m_π close to or above 400 MeV, one of the two σ poles below threshold, although still well isolated, lies somewhat closer to the left cut than to the physical one. Hence, although we will be recasting the full IAM results in terms of our model parameters, up to $m_\pi = 460$ MeV, in the case of the lower mass virtual pole such a simplified description would not be a precise description for pion masses above 400 MeV. Beyond that mass, the description of the lower virtual pole within the simple model should only be considered a qualitative extrapolation. Of course the position of the poles are valid within the approximations of the IAM.

With these caveats in mind, let us now discuss the resulting pole trajectories is some more detail. The pole movement of the σ in the k-plane is shown in the right panel of Fig. 5. Not only provides us the k-plane with a different look at the positions and movements of S-matrix poles, it also allows us to give a simple parameterization for the m_π-dependence of the resonance poles shown in Figs. 4 and 5. Especially we get for the σ

$$\left(k_\mathrm{p}^\sigma\right)^2 = a_\sigma^2\left(b_\sigma^2 - m_\pi^2\right) \quad \text{and}$$
$$\gamma^\sigma = \gamma_0^\sigma + c_\sigma\left(m_\pi/m_\pi^{\mathrm{phys.}}\right)^2, \tag{28}$$

with $a_\sigma = 0.64$ MeV, $b_\sigma = 320.8$ MeV, $c_\sigma = 7.5$ MeV and $\gamma_0^\sigma = 123$ MeV and analogously for the ρ

$$\left(k_p^\rho\right)^2 = a_\rho^2\left(b_\rho^2 - m_\pi^2\right) \quad \text{and}$$
$$\bar{\gamma}\left(k_p^\rho\right)^2 = \gamma_0^\rho + c_\rho\left(m_\pi/m_\pi^{\mathrm{phys.}}\right)^2, \tag{29}$$

with $a_\rho = 0.75$ MeV, $b_\rho = 480$ MeV, $c_\rho = -4.1$ MeV and $\gamma_0^\rho = 44.1$ MeV. A comparison of the fit functions and the full numerical results for the pole movements are shown for the σ and ρ in the left panel of Figs. 5 and 6, respectively. We see that for both k_p and γ very simple two parameter fitting functions provide a reasonable representation of the full results. We start with the physical, non-vanishing values for both γ and k_p for the σ as well as the ρ. As the pion mass gets increased, k_p decreases significantly and eventually vanishes while γ changes relatively little. At the point where $k_\mathrm{p} = 0$, the two poles meet at the real axis below threshold for the σ and exactly at threshold for the ρ, as explained above. When the quark masses are increased further, one σ pole

moves towards the $\pi\pi$ threshold, while the other one moves away from the threshold along the real s (imaginary k) axis.

We can now come back to the discussion of Section 3 and apply the formalism to the σ as derived from the IAM. In case of the σ the range of forces is set by m_ρ. The σ becomes a bound state at $m_\pi = 450$ MeV. At this point we have

$$\gamma \simeq \kappa \simeq 200\ \text{MeV} \to Z \simeq 0.$$

As we have commented, the virtual pole that remains in the second Riemann sheet is now very close to the left cut and its description with the simplified model may not be very precise, but it is clear that the positions of these two poles are so asymmetric with respect to threshold that we can conclude from this analysis that within the IAM, at least for $m_\pi > 450$ MeV the σ is predominantly of molecular nature. Note that, both for simplicity and in order to be conservative, we have shown calculations for the IAM to one-loop from [7], although the two-loop calculation has also been performed [29]. In that case a similar behavior is found, including the appearance of a virtual pole, although for pion masses $m_\pi > 300$ MeV.

Given the large similarity of the pole trajectory of the σ meson and that found for controversial $K(800)$ scalar resonance (or κ) with the IAM using SU(3) ChPT [8], a similar conclusion seems unavoidable for the $K(800)$, especially since the virtual pole predicted as the pion mass increases was recently confirmed in a lattice-QCD calculation [11].

5. Summary

In this paper we discussed on general grounds the properties of pole trajectories as some strength parameter is varied for resonances coupling to the continuum in different partial waves. There is a qualitatively different behavior for states that couple in an s-wave compared to all higher partial waves: only for s-wave states the two, complex conjugate resonance poles on the second sheet meet at some value of the strength parameter below the threshold — for all other partial waves this meeting point is located exactly at threshold. Using Weinberg's compositeness criterion we were able to show that there is a connection between the value of the mentioned subthreshold meeting point and the composition of the wave function of the physical state. To illustrate the mentioned properties we investigated two models: Model A gives hadronic molecules, which one might also call extraordinary hadrons, for all values of the coupling that lead to a pole, while the more general Model B allows for a near threshold state with a prominent elementary component, however, this requires a significant amount of fine tuning.

In lattice QCD resonance poles move as quark masses are varied. Since most simulations at present are still performed at such values of the quark masses/lattice spacings that the resonances cannot decay to the continuum, so-called chiral extrapolations are necessary to relate the lattice results to the real world parameters. For extraordinary s-waves those need to contain striking non-analyticities. This is illustrated in this paper by employing the quark mass dependence of the σ pole as predicted by the inverse amplitude method in combination with one loop chiral perturbation theory. On the basis of this study we were also able to provide a simple parameterization for the pole trajectories that contains the mentioned non-analyticity and should proof useful in future lattice studies.

Acknowledgements

We are particularly thankful towards R.L. Jaffe for his participation at early stages of this work. The research was in part supported by the Spanish project FPA2011-27853-C02-02, DFG funds to the Sino-German CRC 110 "Symmetries and the Emergence of Structure in QCD", and the EU I3HP "Study of Strongly Interacting Matter" under the Seventh Framework Program of the EU.

References

[1] G. 't Hooft, Nucl. Phys. B 72 (1974) 461;
E. Witten, Nucl. Phys. B 160 (1979) 57;
See also E. Witten, Phys. Today 33 (7) (1980) 38.
[2] S. Weinberg, Phys. Rev. Lett. 110 (26) (2013) 261601;
M. Knecht, S. Peris, Phys. Rev. D 88 (2013) 036016.
[3] T.D. Cohen, R.F. Lebed, arXiv:1403.8090 [hep-ph];
T.D. Cohen, R.F. Lebed, Phys. Rev. D 89 (2014) 054018.
[4] T. Cohen, F.J. Llanes-Estrada, J.R. Pelaez, J. Ruiz de Elvira, arXiv:1405.4831 [hep-ph].
[5] N. Brambilla, et al., Eur. Phys. J. C 71 (2011) 1534, arXiv:1010.5827 [hep-ph].
[6] R.L. Jaffe, AIP Conf. Proc. 964 (2007) 1;
R.L. Jaffe, Prog. Theor. Phys. Suppl. 168 (2007) 127, arXiv:hep-ph/0701038.
[7] C. Hanhart, J.R. Pelaez, G. Rios, Phys. Rev. Lett. 100 (2008) 152001, arXiv:0801.2871 [hep-ph].
[8] J. Nebreda, J.R. Pelaez, Phys. Rev. D 81 (2010) 054035, arXiv:1001.5237 [hep-ph].
[9] V. Bernard, M. Lage, U.-G. Meissner, A. Rusetsky, J. High Energy Phys. 1101 (2011) 019, arXiv:1010.6018 [hep-lat].
[10] M. Doring, U.-G. Meissner, E. Oset, A. Rusetsky, Eur. Phys. J. A 47 (2011) 139, arXiv:1107.3988 [hep-lat].
[11] J.J. Dudek, R.G. Edwards, C.E. Thomas, D.J. Wilson, arXiv:1406.4158 [hep-ph].
[12] F. Giacosa, T. Wolkanowski, Mod. Phys. Lett. A 27 (2012) 1250229, arXiv:1209.2332 [hep-ph].
[13] T. Hyodo, arXiv:1407.2372 [hep-ph].
[14] F.-K. Guo, C. Hanhart, U.-G. Meissner, Eur. Phys. J. A 40 (2009) 171, arXiv:0901.1597 [hep-ph].
[15] A.I. Baz', et al., Scattering, Reactions and Decay in Nonrelativistic Quantum Mechanics, IPST, Jerusalem, 1969.
[16] F.-K. Guo, C. Hanhart, F.J. Llanes-Estrada, U.-G. Meissner, Phys. Lett. B 703 (2011) 510, arXiv:1105.3366 [hep-lat].
[17] S. Weinberg, Phys. Rev. 130 (1963) 776;
S. Weinberg, Phys. Rev. 131 (1963) 440;
S. Weinberg, Phys. Rev. 137 (1965) B672.
[18] V. Baru, J. Haidenbauer, C. Hanhart, Yu. Kalashnikova, A.E. Kudryavtsev, Phys. Lett. B 586 (2004) 53, arXiv:hep-ph/0308129.
[19] T. Hyodo, Phys. Rev. Lett. 111 (2013) 132002, arXiv:1305.1999 [hep-ph].
[20] R. Kaminski, L. Lesniak, B. Loiseau, Eur. Phys. J. C 9 (1999) 141, arXiv:hep-ph/9810386;
F. Cannata, J.P. Dedonder, L. Lesniak, Z. Phys. A 334 (1989) 457;
F. Cannata, J.P. Dedonder, L. Lesniak, Phys. Lett. B 207 (1988) 115.
[21] V. Baru, C. Hanhart, Y.S. Kalashnikova, A.E. Kudryavtsev, A.V. Nefediev, Eur. Phys. J. A 44 (2010) 93, arXiv:1001.0369 [hep-ph].
[22] C. Hanhart, Y.S. Kalashnikova, A.V. Nefediev, Eur. Phys. J. A 47 (2011) 101, arXiv:1106.1185 [hep-ph].
[23] E.P. Wigner, Phys. Rev. 98 (1955) 145.
[24] H.-W. Hammer, D. Lee, Phys. Lett. B 681 (2009) 500, arXiv:0907.1763 [nucl-th];
H.-W. Hammer, D. Lee, Ann. Phys. 325 (2010) 2212, arXiv:1002.4603 [nucl-th].
[25] K.A. Olive, et al., Particle Data Group, Chin. Phys. C 38 (2014) 090001.
[26] T.N. Truong, Phys. Rev. Lett. 61 (1988) 2526;
T.N. Truong, Phys. Rev. Lett. 67 (1991) 2260;
A. Dobado, et al., Phys. Lett. B 235 (1990) 134.
[27] A. Dobado, J.R. Peláez, Phys. Rev. D 47 (1993) 4883;
A. Dobado, J.R. Peláez, Phys. Rev. D 56 (1997) 3057;
A. Gomez Nicola, J.R. Pelaez, G. Rios, Phys. Rev. D 77 (2008) 056006.
[28] J.A. Oller, E. Oset, Nucl. Phys. A 620 (1997) 438, arXiv:hep-ph/9702314;
J.A. Oller, E. Oset, Nucl. Phys. A 652 (1999) 407 (Erratum).
[29] J.R. Pelaez, G. Rios, Phys. Rev. D 82 (2010) 114002, arXiv:1010.6008 [hep-ph].